

EVOLUTION OF THE 2002/03 EL NIÑO*

BY MICHAEL J. MCPHADEN

Recent observations highlight how far we have come, and how far we have yet to go, in our ability to understand and accurately predict El Niño.

The El Niño–Southern Oscillation (ENSO) cycle is the most prominent year-to-year climate fluctuation on Earth. It originates in the tropical Pacific with unusually warm (El Niño) and cold (La Niña) events recurring approximately every 3–7 yr. El Niño and La Niña events develop in association with swings in atmospheric pressure between the tropical Indo-Pacific and eastern Pacific. These pressure swings, known as the Southern Oscillation, are intimately related to the strength of the Pacific trade winds. ENSO extends its reach beyond the tropical Pacific through atmospheric teleconnections that affect patterns of weather variability worldwide (see Sidebar 1 on El Niño, La Niña, and the ENSO cycle).

The recent El Niño in 1997/98 was by some measures the strongest of the twentieth century, causing

an estimated \$36 billion worldwide in economic losses and 22,000 fatalities (Office of Global Programs 1999). The United States accounted for about \$4 billion of these losses and nearly 200 fatalities. El Niño is not, however, an unmitigated disaster. Changnon (1999), for example, estimated that many more lives and dollars were saved in the United States during the 1997/98 El Niño because of the reduced number and intensity of landfalling hurricanes in the summer of 1997 and the warmer Midwest temperatures in the winter of 1997/98.

The first El Niño of the twenty-first century occurred in 2002/03. According to standard ENSO indices (Fig. 1), this event was of moderate strength and comparable to El Niños in 1986/87 and 1991/92. As expected, the 2002/03 El Niño affected patterns of global weather variability, though generally less dramatically than either the 1997/98 El Niño or the major El Niño of 1982/83. Among the impacts of the 2002/03 El Niño were drier-than-average conditions over much of Indonesia, northern and eastern Australia, and northeastern South America during the latter part of 2002 and early 2003. Likewise, Indian monsoon rainfalls were deficient in the summer of 2002. Wetter-than-average conditions prevailed over the central equatorial Pacific from mid-2002 to early 2003, the southeastern United States during boreal fall and winter 2002/03, and southeastern South America during September–December 2002. The Pacific Northwest and Alaska experienced an unusually

*Pacific Marine Environmental Laboratory Contribution 2584 and Joint Institute for the Study of the Atmosphere and Ocean Contribution 990

AFFILIATION: MCPHADEN—NOAA/Pacific Marine Environmental Laboratory, Seattle, Washington

CORRESPONDING AUTHOR: Dr. Michael J. McPhaden, NOAA/Pacific Marine Environmental Laboratory, 7600 Sand Point Way NE, Seattle, WA 98115

E-mail: michael.j.mcphaden@noaa.gov

DOI: 10.1175/BAMS-85-5-677

In final form 10 December 2003

EL NIÑO, LA NIÑA, AND THE ENSO CYCLE

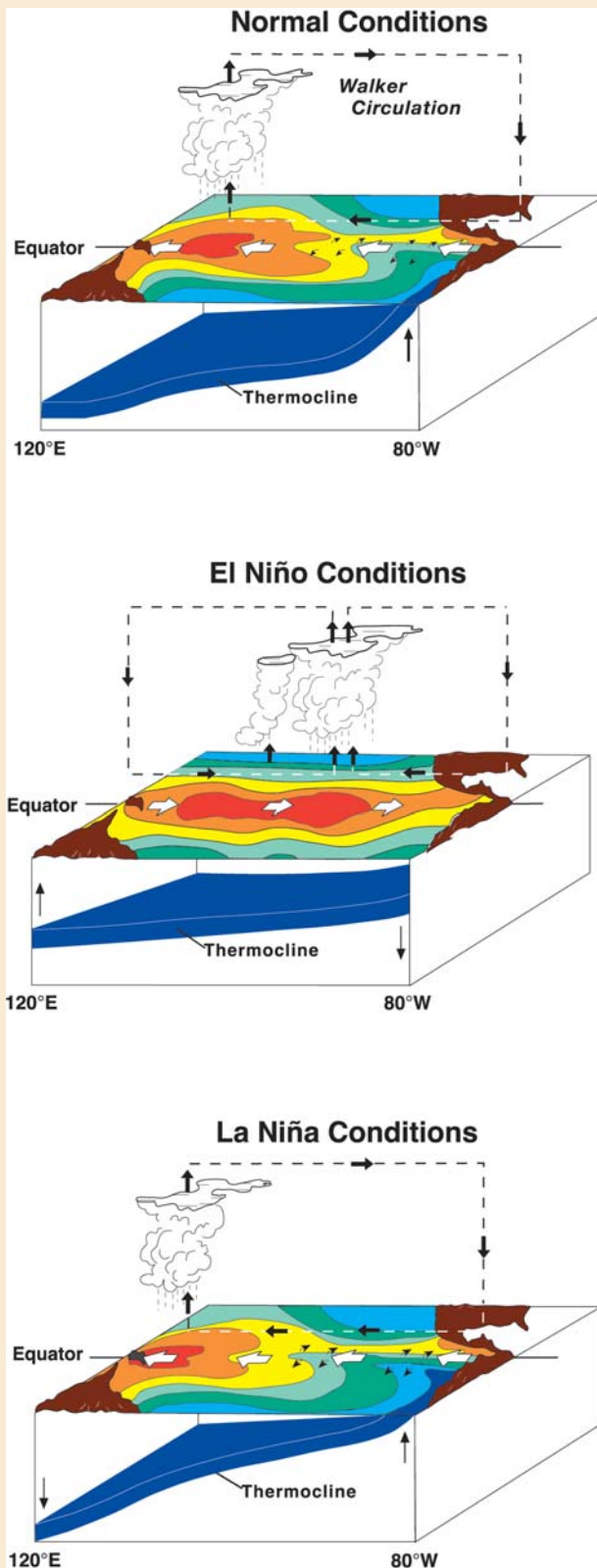


FIG. SBI. Schematic of (top) normal, (middle) El Niño, and (bottom) La Niña conditions.

El Niño and La Niña represent opposite phases of the ENSO cycle, an oscillation of the coupled ocean–atmosphere system between unusually warm and cool conditions in the tropical Pacific. Normally, the trade winds along the equator drive surface flow westward in the South Equatorial Current (Fig. SBI). This current drains surface water heated by the intense tropical sun from the eastern Pacific and piles it up in the western Pacific. The thermocline, which is the region of sharp vertical temperature gradient separating the warm surface layer from the cold deep ocean, is pushed down in the west and elevated in the east. Sea level tends to mirror thermocline depth since sea water expands when heated. Thus, while the thermocline tilts downward toward the west by 100 m along the equator, sea level stands about 60 cm higher in the western Pacific than in the eastern Pacific.

The relative shallowness of the thermocline in the eastern Pacific facilitates the upwelling (i.e., upward transport) of cold interior water by the trade winds, and a cold tongue develops in sea surface temperature from the coast of South America to near the international date line. The east–west surface temperature contrast reinforces the easterly trade winds, since the trades tend to flow down the surface air pressure gradient near the equator and since low atmospheric surface pressure is associated with warm water in the west and high surface pressure with cooler water of the east. Also, as the trade winds flow from east to west, they pick up heat and moisture from the ocean. The warm, humid air mass becomes less dense and rises over the western Pacific warm pool (sea surface temperatures $\geq 28^{\circ}\text{C}$) where deep convection leads to towering cumulus clouds and heavy precipitation. Ascending air masses in this region of deep convection return eastward in the upper levels of the troposphere, then sink over the cooler water of the eastern Pacific. This atmospheric circulation pattern on the equatorial plane is referred to as “the Walker circulation” in honor of Sir Gilbert Walker, who first discovered the Southern Oscillation in the early twentieth century (Bjerknes 1969).

During El Niño, the trade winds weaken along the equator as atmospheric pressure rises in the western Pacific and falls in the eastern Pacific. Weaker trade winds allow the western Pacific warm pool to migrate eastward and the thermocline to flatten out across the basin (Fig. SBI). The ability of upwelling to cool the surface is reduced where the thermocline deepens. Hence, sea surface temperatures warm significantly in the eastern and central equatorial Pacific because of the combination of reduced cooling by upwelling and eastward shifts in the warm pool. El Niño also leads to thermocline deepening and SST warming at midlatitudes along the west coasts of North and South America because of the combined effects of poleward-propagating coastal ocean waves and atmospheric circulation anomalies, both of which are forced from the Tropics.

In the atmosphere, deep cumulus clouds and heavy rains associated with the ascending branch of the Walker circulation normally occur in the western tropical Pacific over the warmest water. As surface temperatures warm to the east during El Niño, convective cloudiness and rainfall migrate eastward toward the date line. This eastward shift in deep convection favors further weakening of the trade winds in the western and central Pacific. Thus, weakening easterlies, eastward shifts in convection, and SST warming tendencies along the equator reinforce one another as El Niño develops (Rasmusson and Wallace 1983).

Eastward shifts in deep convection increase the probability of drought conditions in large parts of Australia, Indonesia, and the Philippines. Conversely, there is a significant increase in the likelihood of torrential rains in the island states of the central Pacific and along the west coast of South America. Tropical rainfall also releases heat into the middle and upper troposphere, providing a source of energy to drive global wind fields. Shifts in these rainfall patterns lead to atmospheric teleconnections, that is, changes in circulation that carry the influence of El Niño to remote parts of the globe, affecting patterns of weather variability worldwide (Trenberth et al. 1998).

The physical oceanographic processes that give rise to El Niño have significant impacts on the biogeochemistry, ecosystems dynamics, and fisheries of the Pacific (Barber and Chavez 1983; Lehody et al. 1997; Chavez et al. 1999). Upwelling brings not only cold thermocline water to the surface, but also water rich in nutrients and inorganic carbon. Thus, biological productivity during El Niño is

generally reduced in the otherwise highly productive equatorial cold tongue and the coastal upwelling zones of the Americas. Sport and commercial fisheries (e.g., salmon, anchoveta, shrimp, and tuna) are susceptible to disruption, marine mammal and sea bird mortality may increase, and coral bleaching can result in areas of prolonged elevated sea temperatures. In addition, the equatorial Pacific normally outgases about one million metric tons of carbon in the form of CO₂ to the atmosphere per year, more than any other region of the World Ocean. During El Niño, there is a reduction in the supply of upwelled carbon to the surface, which leads to a decrease in the flux of CO₂ to the atmosphere (Feely et al. 2002). Thus, El Niño leaves its imprint global carbon cycle through a reduction in the growth of CO₂ in the atmosphere during the early stages of warm events. Conversely, El Niño-related droughts and wildfires release CO₂ from terrestrial carbon reservoirs, accelerating the accumulation of carbon dioxide in the atmosphere during the later stages of warm events (e.g., Page et al. 2002).

The flip side of El Niño, known as La Niña, is characterized by stronger-than-normal trade winds, colder tropical Pacific sea surface temperatures, and a shift in heavy rainfall to the far western tropical Pacific. La Niña often produces effects on global patterns of weather variability that are roughly, though not exactly, opposite to those of El Niño. Its impacts on ocean biogeochemistry are to a first approximation an exaggeration of normal conditions. El Niño and La Niña events typically last 12–18 months and recur roughly every 3–7 yr.

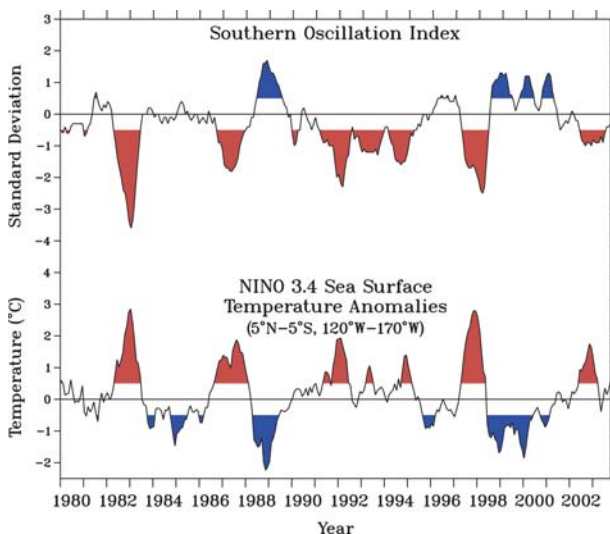


FIG. 1. The Southern Oscillation index (SOI) and Niño-3.4 sea surface temperature index for Jan 1980–Sep 2003. The Niño-3.4 index is computed from monthly SST anomalies in the region 5°N–5°S, 120°–170°W. Positive anomalies greater than 0.5°C indicate El Niño events, and negative anomalies less than –0.5°C indicate La Niña events. The SOI represents an index for the intensity of the easterly trade winds and is computed as a normalized surface air pressure difference between Tahiti, French Polynesia, minus Darwin, Australia, after mean seasonal variations have been subtracted. SOI values have been smoothed with a 5-month running mean for clarity, and periods of SOI greater in magnitude than 0.5 are shaded to emphasize the relationship with El Niño and La Niña. Low SOI is associated with weaker trade winds and warm sea temperatures (El Niño), and high SOI with stronger trade winds and cold sea temperatures (La Niña).

warm 2002/03 winter season. Tropical Atlantic hurricane activity was reduced, as usually happens during El Niño (Pielke and Landsea 1999), with only four hurricanes forming in 2002 compared to eight in typical years since 1995.

Skillful long-range seasonal forecasts provide a basis for developing adaptive strategies that can be implemented to mitigate or take advantage of ENSO-related oceanic and climatic impacts. Much of the skill in long-range weather forecasts over the United States

and elsewhere derives from our ability to predict the evolution of sea surface temperature (SST) anomalies in the equatorial Pacific up to 1 year in advance. While forecasting of ENSO-related tropical Pacific SSTs and their global consequences are far from perfect (Barnston et al. 1999; Mason et al. 1999; Landsea and Knaff 2000), there has nonetheless been significant progress in the development and application of ENSO forecast methodologies over the past 20 yr. As one measure of this progress, V. Kousky of the National Oceanic and Atmospheric Administration (NOAA) Climate Prediction Center (CPC) attributed the success of his group in forecasting the 2002/03 El Niño to “. . . a combination of more experience watching El Niños develop, 2 decades of research, and the observation network that NOAA and NASA have invested in” (Kerr 2002).

Observing and understanding ENSO variability for the purpose of developing skillful climate forecasting capabilities has been a central theme of U.S. and international research programs since the late 1970s. Though much has been learned during this time, there are still many unanswered questions about the nature of El Niño, La Niña, and the ENSO cycle. There is considerable debate at present, for example, about whether ENSO variations result from intrinsic instabilities of the coupled ocean–atmosphere system or whether they are energized primarily by stochastic forcing in the form of weather noise. Likewise, it is unclear at present what determines the limits of ENSO predictability and what those limits are.

The purpose of this paper is to describe the evolution of the 2002/03 El Niño, to illustrate some of the key physical processes at work in its development, and to highlight the degree to which the observed fluctuations are consistent with aspects of ENSO theory. The emphasis here is on the interplay between large-scale low-frequency ocean–atmosphere dynamics and episodic forcing in the form of westerly wind events. Satellite and in situ data and data products derived from the ENSO Observing System (see Sidebar 2) are used for this purpose. Description of the event relies in part on a definition of anomalies relative to climatological mean seasonal cycles. Definition of these anomalies is complicated by the fact that available record lengths for computing climatologies are different for different oceanic and atmospheric variables. However, sensitivity tests indicate that the conclusions are not highly sensitive to the specific years over which the various climatologies are computed.

ONSET AND DEVELOPMENT. The 1997/98 El Niño was followed by a prolonged period of cold

La Niña conditions from mid-1998 to early 2001. The tail end of this La Niña (January–April 2001) can be seen in Figs. 2–4. At this time, stronger-than-normal easterly trade winds prevailed across most of the basin along the equator, while both the western Pacific warm pool (SSTs $\geq 28^{\circ}\text{C}$) and deep atmospheric convection were confined to the west of 160°E (Fig. 2). SSTs in the eastern Pacific were cooler than normal, the westward South Equatorial Current (SEC) was stronger than normal, and the thermocline sloped downward more steeply toward the west (Fig. 3). Sea level, which tends to mirror thermocline depth in the tropical Pacific, rose more steeply to the west, with unusually low sea levels in the eastern basin and unusually high sea levels in the western basin (Figs. 4b and 4c).

La Niña conditions began to weaken in mid-2001 as SSTs warmed near the date line coincident with an increase in episodic westerly wind activity in the western Pacific (Figs. 2 and 3). These westerly winds excited intraseasonal equatorial Kelvin waves, evident as eastward-propagating 1–2-month-long undulations in thermocline depth and South Equatorial Current speed, in the latter half of 2001 and early 2002 (Figs. 3c and 3d). Strong westerly winds in December 2001, in particular, forced a Kelvin wave that depressed the thermocline by 20–30 m, weakened the SEC by as much as 40 cm s^{-1} , and left above-normal SSTs in its wake at all longitudes east of the date line in February–March 2002. At the same time, cooling of the warm pool west of 160°E occurred in association with locally intensified surface wind speeds. As a result, the large-scale zonal SST gradient weakened along the equator and deep atmospheric convection extended eastward toward the date line (Figs. 2b and 2c).

Motivated by the abrupt oceanic and atmospheric changes that occurred in association with the westerly wind event in December 2001, NOAA issued an advisory on 10 January 2002 stating, “. . . warming is being observed over the Tropical Pacific, which could lead to an El Niño by early Spring . . .” (online at www.noaa.gov/news/stories/s849.htm). It was surprising to many therefore that the oceanic response to the strong December 2001 westerly wind burst was short-lived and that conditions returned to near-normal across the basin by April 2002. Uncertainty about how events would unfold in the tropical Pacific was evident in an advisory issued by the World Meteorological Organization on 27 March 2002 stating, “Differing computer models still vary on whether the situation will develop further into . . . an El Niño [though] the large-scale situation remains favorable . . .”

THE ENSO OBSERVING SYSTEM

The ENSO Observing System was developed as a multinational effort during the 10-yr (1985–94) Tropical Ocean Global Atmosphere (TOGA) Program (McPhaden et al. 2001). A key feature of the observing system is the real-time delivery of oceanographic and surface meteorological data for monitoring of evolving climatic conditions, scientific analyses, and ENSO forecasting. The system was designed with emphasis on the ocean, which was very sparsely sampled and for which no equivalent, such as the World Weather Watch, existed. In situ components consist of the Tropical Atmosphere Ocean/Triangle Trans-Ocean Buoy Network (TAO/TRITON) array of moored buoys, an array of drifting buoys, a ship-of-opportunity program, and a network of island and coastal sea level measurement stations (Fig. SB2). Profiling float data are being incorporated into the data stream as the new Argo program (Argo Science Team 2001) becomes established. Complementing this suite of ocean-based measurements is a constellation of earth-observing research and operational satellites.

In terms of measurement priorities, the ENSO Observing System emphasizes large-scale coverage for surface winds, SST, upper-ocean temperatures and currents, and sea level. Surface wind stress and sea surface temperature mediate coupling of the ocean and atmosphere in the Tropics. The multiseason evolution of ENSO is controlled in part by the propagation of large-scale equatorial waves that redistribute upper-ocean heat content in the Pacific basin. Thus, predictability for the ENSO cycle is to be found in the slow evolution of upper-ocean heat content, providing the logic for initializing ocean models used in climate prediction with subsurface temperature data. The tropical oceans behave in many ways as a two-layer fluid, with thermocline variations reflected in sea level heights. Sea level thus provides a convenient proxy of upper-ocean heat content and a measure of the vertically integrated oceanic response to atmospheric forcing. Measurement of

ocean currents is essential because of the strong control ocean dynamics plays in generating ENSO SST anomalies.

In addition to these variables there is a growing appreciation for the importance of improving the characterization of air–sea heat fluxes that affect the surface layer temperature balance (Weller and Anderson 1996). Likewise, coupling between the upper-ocean heat and salt balances in the Tropics has highlighted the possible role of salinity in affecting ENSO variability and predictability (Maes et al. 2002; Ballabrera-Poy et al. 2002). The western and central equatorial Pacific are characterized by large interannual variations in surface and subsurface salinity that affect vertical buoyancy gradients and the formation of salt stratified barrier layers (Lukas and

Lindstrom 1991; Ando and McPhaden 1997). Barrier layers in turn can affect the vertical distribution of turbulent energy, the storage of heat in the upper ocean, and the evolution of SST. Salinity also affects sea level variability, pressure gradients, and therefore ocean current dynamics. Thus, increased effort has been placed on the accurate determination of salinity and surface freshwater flux forcing due to precipitation in the tropical Pacific.

The ENSO Observing System represents a contribution to the Global Ocean Observing System (GOOS) and the Global Climate Observing System (GCOS), programs intended to coordinate international contributions to sustained observations for operational and research purposes.

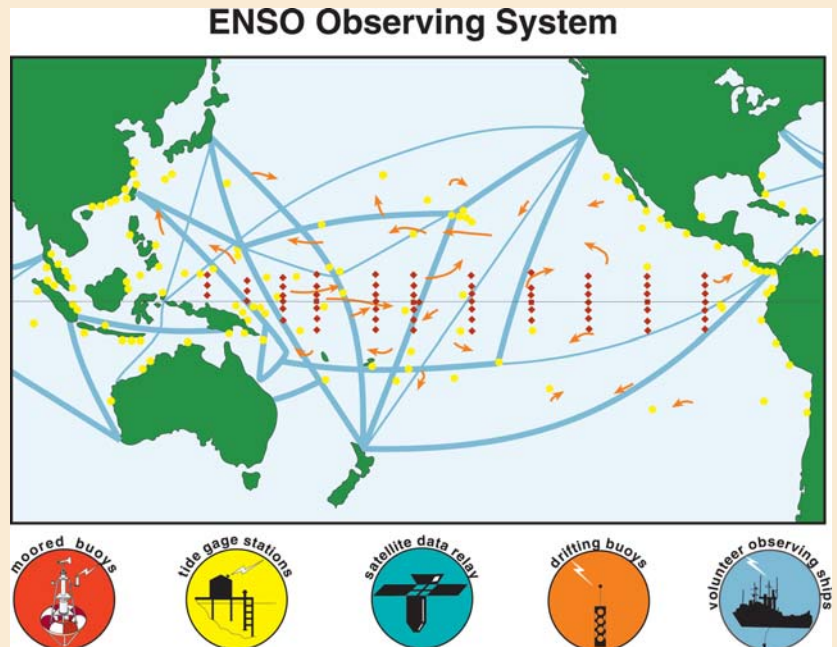


FIG. SB2. In situ components of the ENSO Observing System. The four major elements of this observing system are 1) a ship-of-opportunity program for ocean temperature profiles and surface marine meteorological observations (shown by schematic blue ship tracks); 2) an island and coastal tide gauge network for sea level measurements (yellow circles); 3) a drifting buoy network for sea surface temperatures and ocean currents (shown schematically by curved orange arrows); and 4) a moored buoy array for wind, ocean temperature, and ocean current measurements (red symbols). One schematic drifting buoy arrow represents 10 actual randomly distributed drifters. Not shown are Argo profiling floats that are being deployed in increasing numbers throughout the Tropics or the constellation of operational and research satellites that provide critical space-based measurements. Most data from the in situ components of the observing system are transmitted to shore within hours of collection via satellite.

Five-day Zonal Wind, SST, OLR and Ten-day Zonal Currents Along the Equator

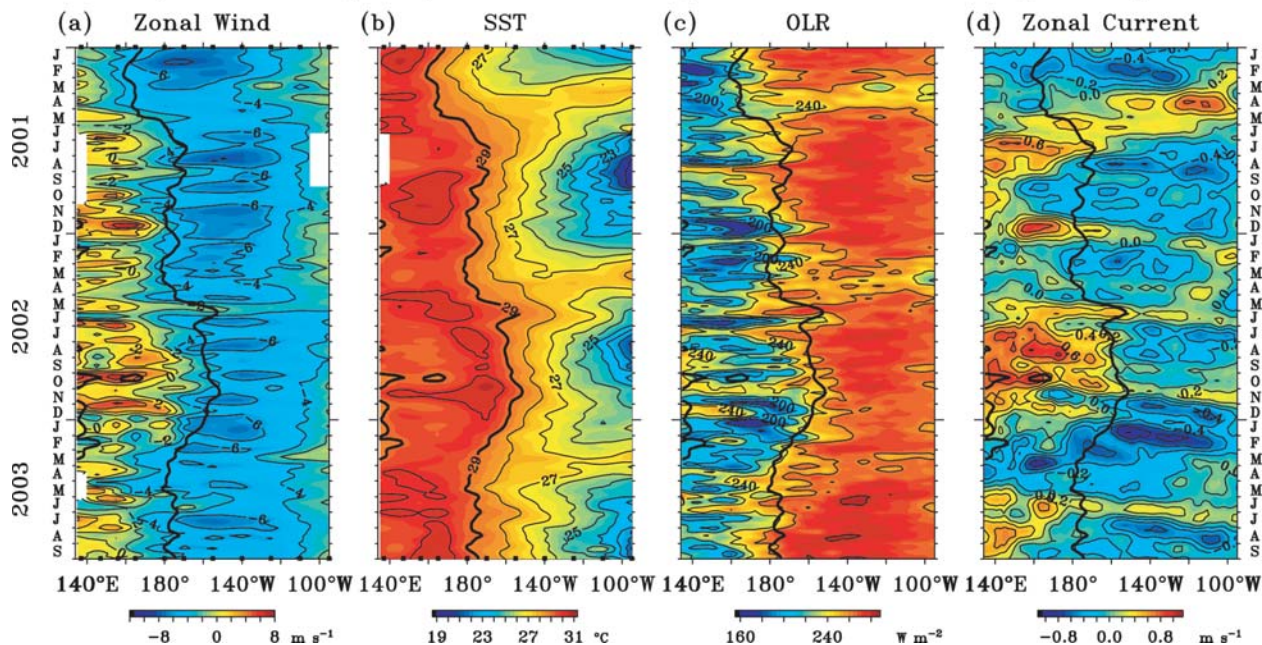


Fig. 2. Five-day analyses of (a) zonal wind and (b) SST averaged between 2°N–2°S based on TAO/TRITON moored time series data. (c) Outgoing longwave radiation (OLR; a measure of high convective cloudiness and rainfall in the Tropics) averaged between 5°N–5°S and based on NOAA’s polar-orbiting weather satellites. (d) Ten-day zonal velocity averaged between 2°N–2°S based on a diagnostic model using sea level data from the TOPEX/Poseidon and Jason satellite altimeters, wind and SST data from satellites, and climatological hydrographic data (Bonjean and Lagerloef 2002). Overplotted on (a), (c), and (d) is the 29°C isotherm from (b). Ticks on the axis of (a) and (b) indicate longitudes sampled at the (top) start and (bottom) end of record. The 10-day temporal resolution in (d) is determined by the approximate 10-day repeat orbit of the satellite altimeters.

Five-day Zonal Wind, SST, 20°C Depth Anomalies and Ten-day Zonal Current Anomalies Along the Equator

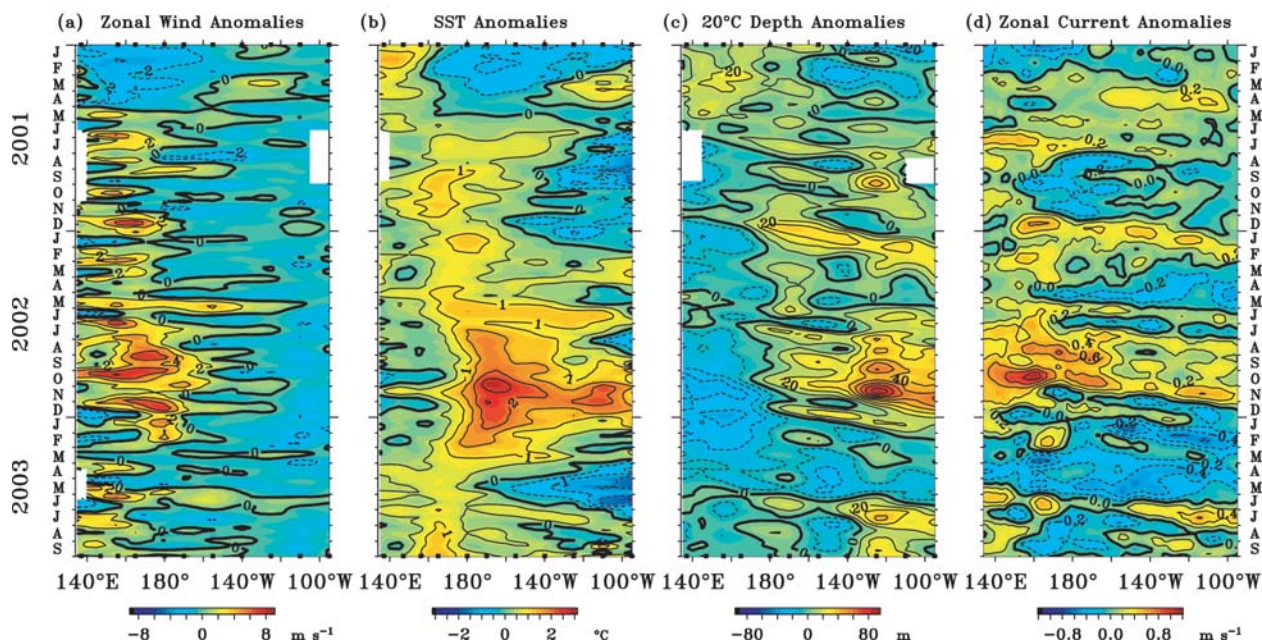


Fig. 3. Five-day average anomalies of (a) zonal wind, (b) SST, and (c) 20°C depth (an index for the depth of the thermocline) relative to the mean seasonal cycle averaged between 2°N–2°S based on TAO/TRITON moored time series data. (d) Ten-day zonal velocity anomalies averaged between 2°N–2°S relative to the mean seasonal cycle. Velocity is based on a diagnostic model as described in the caption to Fig. 2. Ticks on the axis of (a)–(c) indicate longitudes sampled at the (top) start and (bottom) end of record. The 10-day temporal resolution in (d) is determined by the approximate 10-day repeat orbit of the satellite altimeters. Anomalies are relative to climatologies based on data for SST from 1971 to 2000 (Xue et al. 2003), for winds from 1946 to 1989 (Woodruff et al. 1987), for 20°C isotherm depth from 1970 to 1991, and for surface currents from 1993 to 2001.

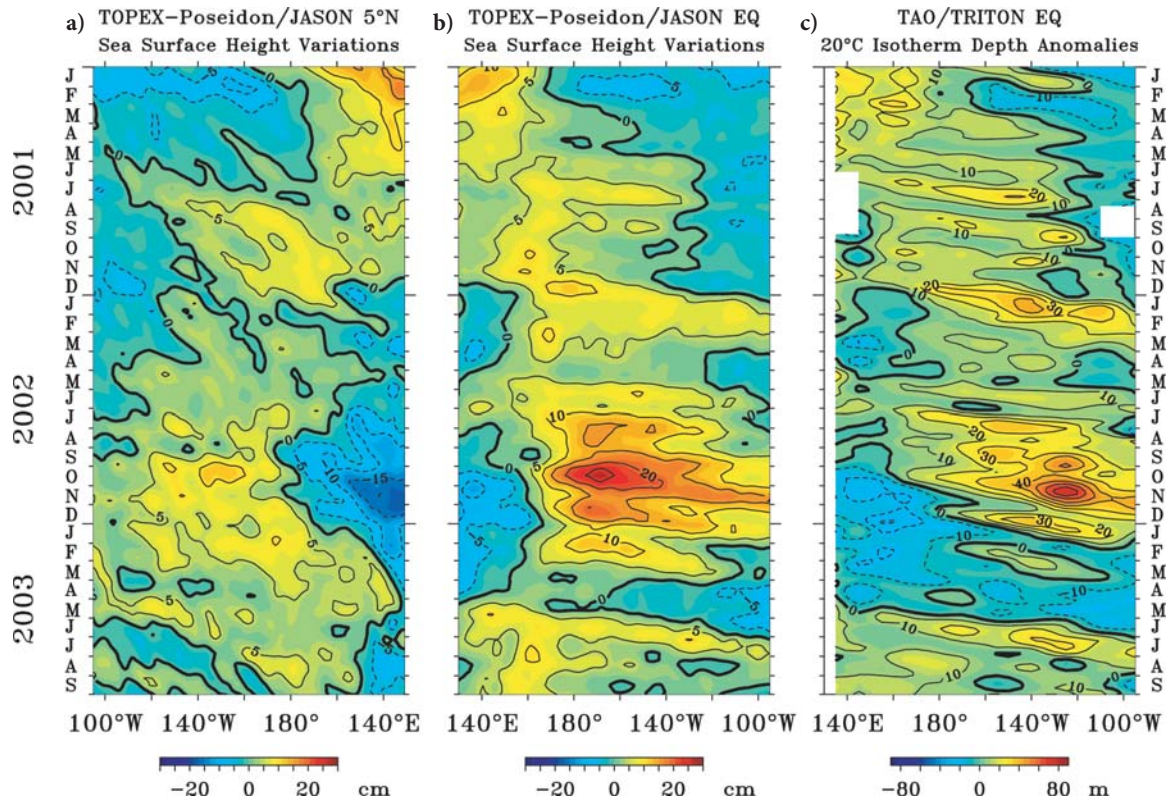


Figure 4. Ten-day anomalies of sea level from a 1° lat/long analysis of TOPEX/Poseidon and Jason altimeter data along (a) 5°N and (b) averaged between 2°N – 2°S . Panel (c) shows 5-day 20°C isotherm depth anomalies averaged between 2°N – 2°S . Anomalies are relative to climatologies based on data from 1993–2001. The longitudinal axis has been reversed in (a) to show connectivity of westward propagating anomalies along 5°N reflecting into eastward propagating anomalies along the equator. Similarities between panels (b) and (c) indicate the tendency for variations in sea level to mirror those in thermocline depth in the equatorial Pacific. Note however that sea level anomalies along the equator in the central Pacific are much larger in late 2002 and less negative in early 2003 than thermocline depth anomalies most likely because of the effects of unusually fresh equatorial mixed layers salinities on sea level (see text for discussion). Also note that differences between panel (c) and Fig. 3c indicate how the definition of anomalies can quantitatively (though not qualitatively) change depending on the years chosen to compute climatologies.

Then in May, an abrupt relaxation of the trade winds extending all the way to 140°W led to basin-scale warming of over 1°C . Confidence that El Niño would develop increased such that the International Research Institute declared on 17 June 2002, . . . there is a 75% probability of an El Niño in 2002 . . . and its strength is most likely to be weak . . .” (<http://iri.columbia.edu/climate/cid/jun2002/>). At the time of this announcement, another westerly wind burst was developing in the western Pacific; it lasted through early July and helped to sustain the warming that began in May. On 11 July 2002 NOAA declared, “It’s official now: El Niño is back . . .” (www.noaa.gov/stories/s938.htm).

The latter half of 2002 witnessed the amplification of both oceanic and atmospheric anomalies associated

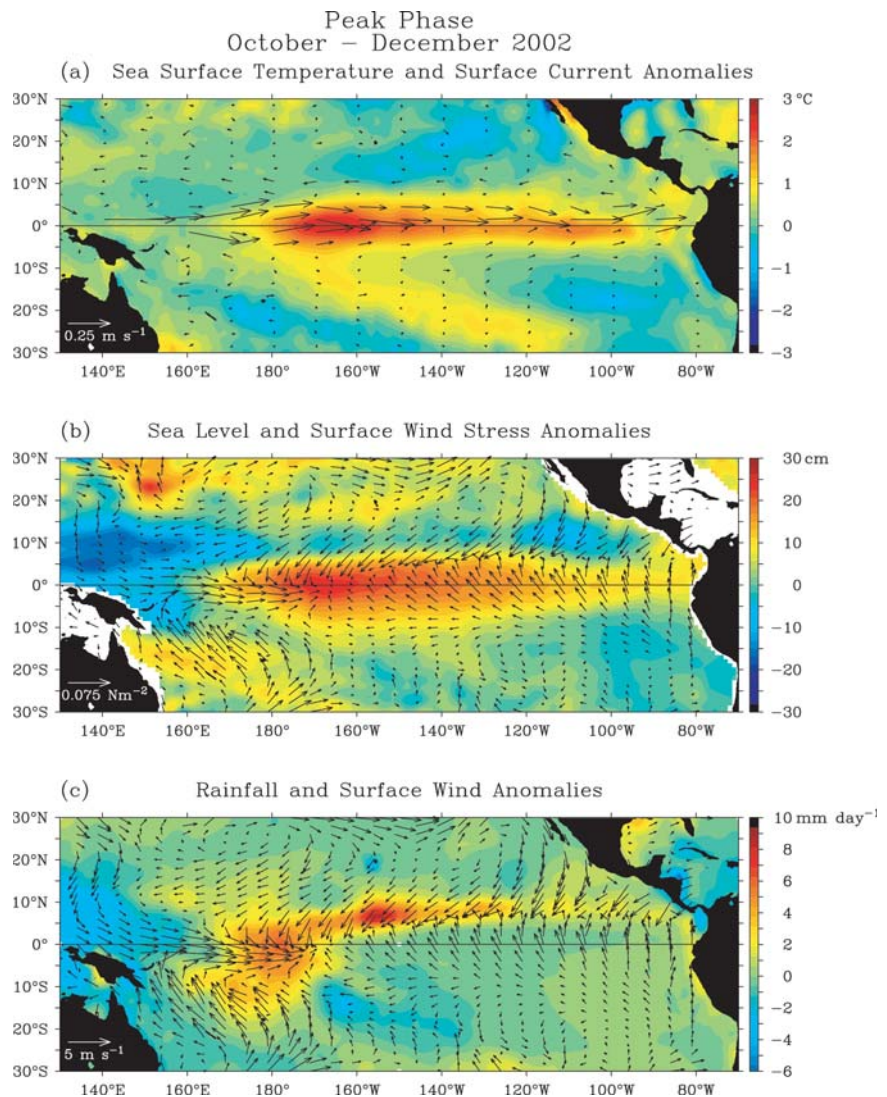
with El Niño. Anomalous westerly wind forcing continued to excite equatorial Kelvin waves that depressed the thermocline and elevated sea level as they propagated eastward. Downwelling associated with these remotely forced Kelvin waves contributed to sustained growth of warm SST anomalies in the eastern Pacific cold tongue. Westerly winds also drove intense eastward currents along the equator (Fig. 2d), advecting the western Pacific warm pool into the central Pacific (Lagerloef et al. 2003). Thus, the 29°C isotherm (near the eastern edge of the warm pool) extended 2000–3000 km to the east of the date line during the second half of 2002 (Fig. 2). In the western Pacific, anomalous westerlies generated westward-propagating upwelling Rossby waves that elevated the thermocline and depressed sea level

(Fig. 4a). SSTs decreased in the western Pacific (Fig. 3b) as the thermocline shoaled to facilitate turbulent vertical transport of cold water from the ocean interior to the surface, and as wind speed-mediated latent cooling intensified. Resultant changes in equatorial SSTs reinforced the eastward expansion of atmospheric deep convection so as to sustain the developing El Niño conditions.

PEAK PHASE. El Niño anomalies peaked for most oceanic and atmospheric variables (e.g., equatorial SST, zonal wind, eastern Pacific thermocline depth) during October–December 2002 or slightly later (e.g., January 2003 for deep convection and rainfall near the date line). The Niño-3.4 SST anomalies (i.e., averages over 5°N–5°S, 120°–170°W) reached 1.8°C in Novem-

ber 2002, approximately equal to peak values during the moderate-strength 1986/87 and 1991/92 El Niños (Fig. 1) and larger than expected from forecasts during the early stages of the event. Largest SST anomalies were concentrated in the central equatorial Pacific, with localized maxima over 2.5°C near 170°W (Figs. 2b and 5a). Conversely, SST anomalies were relatively weak and short-lived in the eastern Pacific and along the west coasts of the Americas (Fig. 5a). The spatial pattern of anomalies resembled that observed during the 1994/95 El Niño but contrasted that of the 1997/98 El Niño and most previous events (Rasmusson and Carpenter 1982; Harrison and Larkin 1998). Typically, largest SST anomalies are concentrated farther east along the equator and coastal warmings are more pronounced.

FIG. 5. Charts showing Oct–Dec 2002 anomalies relative to climatological Oct–Dec means for (a) SST and surface currents, (b) sea level and surface wind stress, and (c) rainfall and surface wind velocity. SST is based on a 1° lat/lon blended satellite/in situ analysis from Reynolds et al. (2002), sea level is a 1° lat/lon analysis of TOPEX/Poseidon and Jason satellite altimeter data (Lagerloef et al. 1999), surface wind velocity and wind stress are from a 1° lat/lon analysis of the QuikSCAT scatterometer (Pegion et al. 2000), rainfall based on a 2.5° lat/lon means of precipitation derived from station gauges and satellite estimates (Janowiak and Xie 1999), and surface currents are from a 1° lat/lon analysis of satellite and in situ data (Bonjean and Lagerloef 2002). Wind velocity and wind stress anomalies are computed relative to a scatterometer climatology from European Remote Sensing satellites (Bentamy et al. 1996) for 1992–2000, sea level and surface current anomalies are relative to a 1993–2001 climatology, SST anomalies are relative to a 1971–2000 climatology, and rainfall anomalies are relative to a 1979–95 climatology. QuikSCAT wind stress has been calculated assuming a drag coefficient of 1.2×10^{-3} and an air density of 1.2 kg m^{-3} . Vectors fields are drawn at reduced resolution for clarity.



Westerly wind velocity and wind stress anomalies along the equator in the western Pacific were also the largest on average between October and December 2002 (Figs. 5b and 5c), with seasonal means over some areas west of the date line of about 5 m s^{-1} and 0.04 N m^{-2} , respectively. Highest sea level anomalies along the equator occurred in the central Pacific near 170°W (+25 cm) associated with a deep surface layer warm-water pool (Fig. 6) in a region of anomalous trade wind convergence. Sea levels were depressed by 10–20 cm in the far western Pacific between 10°S and 15°N , where equatorial Rossby wave influences are expected to be largest and where off-equatorial wind stress curl anomalies favored local upwelling and lower sea levels (Fig. 5b).

In response to the weakened trade winds along the equator in the western and central Pacific, the thermocline deepened on average by 30–40 m in the east and shoaled by 20–30 m in the west such that its slope (as measured by the 20°C isotherm depth) was essentially flat between 140°W and 140°E (Fig. 6). Anomalous eastward currents along the equator (Fig. 5a) supplied the mass flux needed to balance these thermocline depth changes. As occurs at the height of many El Niño events, zonal wind stress in the eastern Pacific along the equator was somewhat stronger than normal, with anomalous easterlies prevailing between about 90° – 160°W in October–December 2002 (Fig. 5b). Easterlies along the equator favor local upwelling. However, because the thermocline was deeper than normal in the eastern Pacific at this time, water upwelled to the surface was unusually warm, resulting in the development of warm SST anomalies.

Heavy rains near the date line and unusually dry conditions in the far-western Pacific during the peak phase of the El Niño (Fig. 5c) were associated with an eastward shift in the ascending branch of the Walker circulation in tandem with an eastward expansion of the warm pool (Fig. 2b). A band of anomalous rainfall also ran east–west between 5° and 10°N in the central and eastern Pacific, indicating an equatorward shift of the intertropical convergence zone (ITCZ) in response to the unusually warm equatorial SST anomalies (Rasmusson and Carpenter 1982; Janowiak and Xie 1999). The ITCZ rainfall anomalies were most pronounced in the central Pacific and, like the SST anomalies, tapered off toward the east. Rainfall anomalies near the date line and in the ITCZ were associated with anomalous surface wind convergence, while the unusually dry zone in the western Pacific was associated with anomalous surface zonal wind divergence near the equator. In the Southern Hemisphere, rainfall anomalies were linked to changes in

Quarterly TAO/TRITON Temperatures ($^\circ\text{C}$) 2°S to 2°N Average

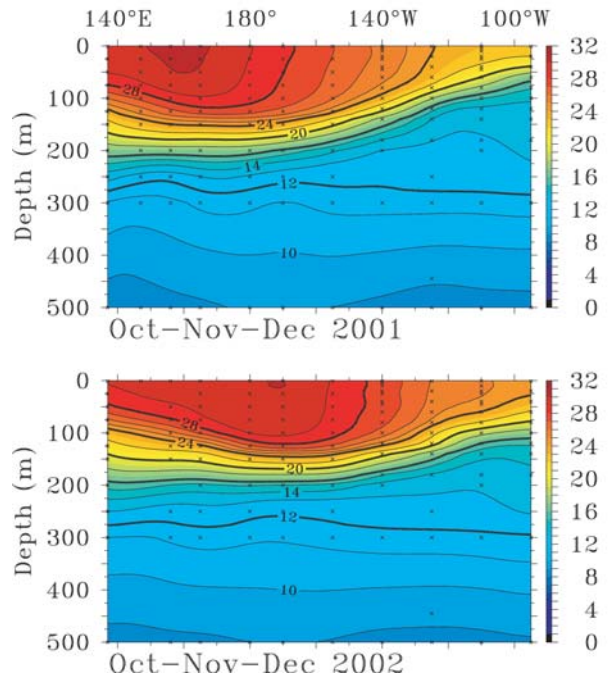


FIG. 6. Zonal section of temperatures averaged between 2°N and 2°S based on TAO/TRITON time series for (top) Oct–Dec 2001 and (bottom) Oct–Dec 2002. Longitudes and depths with data are indicated by x's. Contour interval is 2°C between 16° and 24°C and 1°C otherwise.

the location and intensity of the South Pacific convergence zone (SPCZ).

The western Pacific warm pool is characterized not only by high SSTs ($\geq 28^\circ\text{C}$) but also by low surface salinities ($< 35 \text{ psu}$) because of heavy convective rains in the region associated with the ascending branch of the Walker circulation. Eastward expansion of the warm pool during El Niño therefore results in both warming and freshening of the central Pacific (Delcroix and Picaut 1998; Delcroix and McPhaden 2002). Mixed layers in this region also tend to be relatively shallow because heavy rains and vertically sheared currents lead to the formation of strong vertical salinity gradients that control near-surface density stratification (Ando and McPhaden 1997; Cronin and McPhaden 2002). Below these mixed layers there is typically a layer of relatively uniform temperature that separates the surface from the thermocline. This intervening layer is referred to as the “barrier layer” because it impedes turbulent vertical exchange of heat between the warm surface and the cold thermocline below (Lukas and Lindstrom 1991). This insulating property of barrier layers can enhance SST warming

by trapping heat gained from the atmosphere in shallow surface mixed layers. Thus, the potential exists for salinity variations to feed back indirectly to the atmosphere through SST, affecting ENSO variability and predictability (Maes et al. 2002).

Interannual changes in upper-ocean water mass properties during the 2002/03 El Niño are illustrated from two shipboard conductivity–temperature–depth (CTD) sections separated by 1 yr in the central Pacific (Fig. 7). Between November 2001 (prior to the onset of the El Niño) and October–November 2002 (at the peak of the El Niño), there was a drop in salinity of over 1 psu between 5°N and 5°S in the upper 50 m of the water column. Corresponding density

sections (Fig. 7) indicate the formation of a very shallow surface mixed layer in October–November 2002 in which temperatures above 30°C are found. This mixed layer results primarily from salt stratification and appears to be well separated from the thermocline. Time series from TAO/TRITON moorings along the equator also show unusually low surface salinities in the central Pacific like those in Fig. 7 from mid-2002 to early 2003. Thus, it is plausible that trapping of heat in shallow salinity-stratified surface mixed layers and reduction of turbulent vertical exchange with the thermocline may have helped to boost SST anomalies in the central Pacific during the 2002/03 El Niño (Fig. 5a).

Low surface salinities, because of their effect on density, also contributed several centimeters to equatorial sea level elevations in the central Pacific during the El Niño. In the case of the October–November 2002 CTD section, for example, the drop in near-surface salinity between 5°N and 5°S led to an additional 3–7 cm of sea level elevation over what would have been expected had average surface water mass properties prevailed (Fig. 7). These salinity-induced changes in sea level were in addition to those resulting from equatorial wave variations and other dynamical processes (Figs. 4b and 4c).

DEMISE. Following peak conditions in late 2002–early 2003, the El Niño began to wane as indicated by weakening SST, thermocline depth, zonal wind, and other oceanic and atmospheric anomalies. A gradually shoaling thermocline and falling sea level extended eastward along the equator beginning in late 2002, qualitatively consistent with the reflection of upwelling Rossby waves

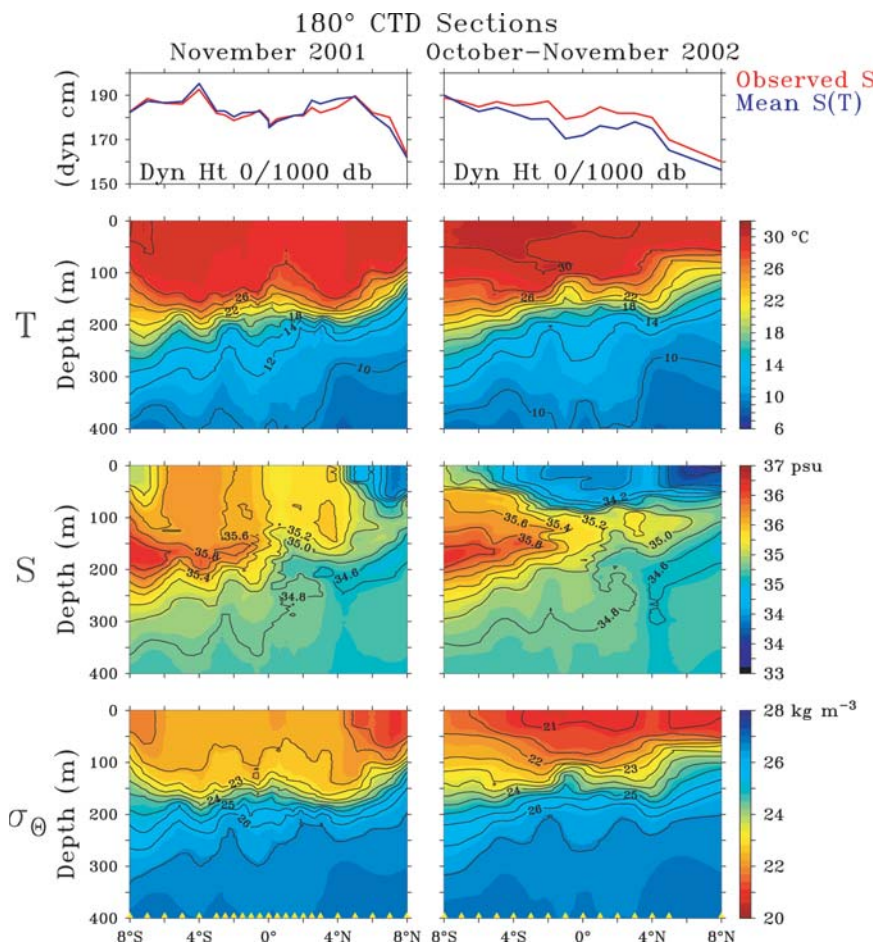


FIG. 7. Meridional sections of (top) temperature (T), (middle) salinity (S), and (bottom) potential density (σ_{θ}) along 180° longitude based on CTD measurements collected from cruises of the NOAA ship *Ka'imimoana* during (left) 10–17 Nov 2001 and (right) 23 Oct–17 Nov 2002. Yellow triangles along the bottom axis of the potential density sections indicate the locations of CTD stations. Also shown is dynamic height of the sea surface (in dynamic cm) relative to 1000 m using observed temperatures and salinities (red curves) and observed temperatures but salinity based on climatological temperature–salinity relationships (blue curves). Dynamic height variability is nearly identical to that for sea level in the Tropics at subtidal frequencies.

into upwelling equatorial Kelvin waves at the western boundary (Fig. 4). These reflected waves provide the delayed negative feedback that eventually brings an end to El Niño according to delayed oscillator theory (Battisti 1988; Schopf and Suarez 1988). However, thermocline shoaling at this time was also in part related to upwelling Kelvin waves directly forced by anomalous easterly winds in the far western Pacific (Figs. 3a and 3c), as observed during the termination phase of previous El Niños (e.g., Weisberg and Wang 1997; McPhaden and Yu 1999; Boulanger et al. 2003; Harrison and Vecchi 1999). Additional cooling tendencies involved anomalous westward flow along the equator (Fig. 3d) related to wind-forced and/or western-boundary-generated upwelling Kelvin waves and possibly to eastern-boundary-generated Rossby waves (e.g., Picaut et al. 1996, 1997). The observed anomalous westward flows contributed to contraction of the western Pacific warm pool as evident in the westward migration of the 29°C isotherm during January–April 2003 (Fig. 2).

By early May 2003, warm SST anomalies were reduced to only about 0.5°C and confined to west of the date line, while cold SST anomalies over 1°C had emerged in the eastern equatorial Pacific. Lingering convective anomalies near the date line were also greatly reduced in amplitude. These trends in large-scale conditions prompted NOAA to issue an advisory on 19 May 2003 stating, “. . . it is likely that La Niña will develop over the next few months.” However, at the time of this announcement, a westerly wind burst was developing in the western Pacific (Fig. 3). This wind burst generated a downwelling Kelvin wave—strikingly evident at sea level, 20°C isotherm depths, and zonal currents along the equator—that led to the reemergence of weak warm-SST anomalies all across the basin in June–July 2003 (Figs. 3 and 4). The May wind burst was followed by another weaker westerly wind event in July 2003 that helped to further arrest evolution toward La Niña. By September 2003, near-neutral rather than La Niña conditions prevailed (Fig. 1), with warm 1°C anomalies lingering near 170°E (Fig. 3b).

HEAT CONTENT VARIATIONS. ENSO variability is intimately linked to alternating stages of oceanic heat content buildup and discharge from equatorial latitudes (Wyrтки 1985; Cane et al. 1986; Zebiak 1989). These heat content variations are mediated by wind-forced equatorial waves and affect SST through equatorial upwelling and other processes. Changes in SST then feed back to the atmosphere to modify surface wind and precipitation patterns. The slow sea-

sonal evolution of upper-ocean heat content and its feedbacks to the atmosphere accounts for the characteristic interannual time scale of ENSO. The predictability of ENSO likewise derives from the deterministic wind-driven ocean dynamics that govern this slowly evolving upper-ocean thermal field.

In his “recharge” oscillator theory, Jin (1997) synthesized much of the early work on the importance of oceanic heat content variations in the ENSO cycle. According to this theory 1) a buildup of excess heat content along the equator is a prerequisite for the occurrence of El Niño; 2) the equatorial Pacific is purged of excess heat content during El Niño; and 3) the time between El Niños is determined in part by the time it takes to recharge equatorial latitudes with excess heat once again. Empirically it has also been determined that the magnitude of El Niño SST anomalies usually scales in proportion to the magnitude of the prior heat content buildup (Meinen and McPhaden 2000).

Zonally integrated heat content along the equator provides a convenient index for interpreting ENSO variability in terms of recharge oscillator theory. Our definition of heat content for this purpose is the integrated warm water volume (WWV) above the 20°C isotherm between 5°N and 5°S from the eastern to the western boundary of the Pacific (Meinen and McPhaden 2000). The lower boundary for this integration is the depth of the 20°C isotherm, which is located in the middle of the upper thermocline (q.v. Fig. 6). The 5°N–5°S latitudinal range is chosen to maximize the zonally coherent accumulation and loss of warm water along the equator on ENSO time scales.

It is evident from the WWV time series and the Niño-3.4 SST index (Fig. 8) that a buildup in heat content along the equator has preceded all El Niños since 1980 by two to three seasons. The heat content buildup prior to the 2002/03 El Niño was about half that prior to 1997/98, and comparable to that prior to the 1986/87 and 1991/92 El Niños. Based on this heat content precursor, one would have expected maximum Niño-3.4 SST anomalies for the 2002/03 El Niño to be significantly smaller than those in 1997/98 and similar to those in 1986/87 and 1991/92.

WWV along the equator peaked in September 2002, after which it began to rapidly decrease, in accordance with the idea that El Niño should purge excess heat from the equatorial band (Fig. 8). WWV became weakly negative in February–April 2003, consistent with the existence of a shallower-than-normal thermocline along the equator at that time (Fig. 3c). The steep plunge in WWV from September 2002 to

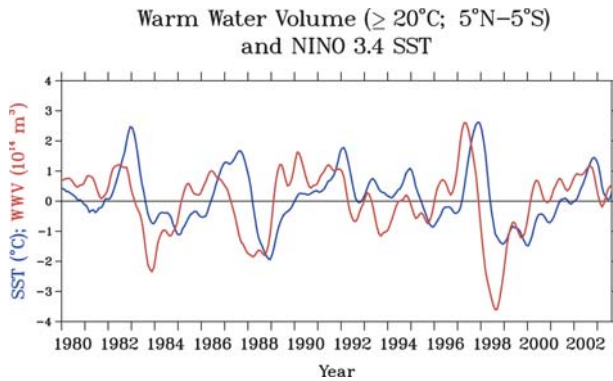


FIG. 8. Monthly anomalies of WWV (5°N–5°S, 80°W–120°E above the 20°C isotherm) and Niño-3.4 SST (5°N–5°S, 120°–170°W) from Jan 1980 to Sep 2003. WWV is based on a blended analysis of TAO/TRITON moored time series data and ship-of-opportunity expendable bathythermograph (XBT) data (Smith 1995). Time series have been smoothed with a 5-month running mean filter for display (after Meinen and McPhaden 2000).

February 2003 was a harbinger of El Niño's demise in boreal spring, though WWV subsequently rebounded to positive values in mid-2003 in response to renewed episodic westerly wind forcing.

This description illustrates the utility of upper-ocean heat content as a precursor of ENSO time-scale SST variations. However, a close inspection of Fig. 8 also reveals some apparent inconsistencies. The heat content deficit along the equator following the 1997/98 El Niño took about 2 yr to disappear. A substantial excess of heat content eventually developed in early 2000 and, after declining in midyear, reemerged again in early 2001. An El Niño did not develop in either 2000 or 2001, however, even though the excess heat content early in both years was nearly equal to that in early 2002. Other years have shown the promising development of heat content precursors (such as 1989 and early 1990) that did not lead immediately to the development of El Niño events. These results suggest that while heat content buildup along the equator may be a necessary condition for El Niño to occur, it is not a sufficient condition. So while the ocean may be otherwise poised for the onset of a warm event based on integrated ocean heat content, other factors must contribute to the development of El Niño. These factors may involve large-scale mutually reinforcing patterns of wind and SST variability and/or weather noise in the form of episodic atmospheric forcing.

ENSO STABILITY CHARACTERISTICS. El Niño can be understood in part through a set of

circular arguments involving positive feedbacks between the ocean and the atmosphere: a weakening of the trade winds causes surface warming along the equator, while surface warming leads to eastward shifts in deep convection that produce further weakening of the trade winds. A similar set of arguments involving strengthening trades, westward shifts in convection, and cooling surface temperatures apply to La Niña. Positive feedbacks between surface zonal winds, SST, and atmospheric deep convection over the western Pacific warm pool as illustrated in Sidebar 1 were evident throughout the 2002/03 El Niño (Fig. 2). For example, the seasonal envelope of deep convection migrated zonally with the warmest surface waters. Likewise, westerly winds in the surface layer inflow region to the west of the convection expanded and contracted with east–west displacements of the warm pool.

A fundamental question is whether these large-scale feedbacks are strong enough to result in an ENSO cycle that is unstable, with self-sustaining natural oscillations between unusually warm and cold conditions (Jin 1997; Neelin et al. 1998). Under these circumstances, ENSO predictability would be limited primarily by noise in initial conditions as with weather prediction. On the other hand, weaker feedbacks between the ocean and the atmosphere would result in a stable or damped ENSO cycle better characterized as a series of discrete warm events punctuating periods of neutral or unusually cold conditions. For a damped ENSO cycle, stochastic atmospheric forcing associated with weather variability would then be required to initiate and sustain individual El Niño events. Weather phenomena are unpredictable more than about 2 weeks in advance. Hence, on seasonal-to-interannual time scales they represent noise that can be a major limitation to predictability of ENSO (Kleeman and Power 1994; Eckert and Latif 1997; Moore and Kleeman 1999; Kirtman and Schopf 1998). Weather variability takes many forms in the tropical Pacific such as wind fluctuations associated with the Madden–Julian oscillation (MJO), generic westerly wind bursts, cold air outbreaks from midlatitudes, and tropical cyclones (Keen 1982; Madden and Julian 1994; Harrison and Vecchi 1997; Yu and Reinecker 1998). All have the potential to introduce irregularity into the amplitude, duration, and seasonal phasing of ENSO variations.

Theory indicates that the system may be damped, stable, or unstable, depending on the large-scale oceanic and atmospheric background conditions on which ENSO develops (Fedorov and Philander 2000). Arguments have been marshaled to support the full

range of possibilities using statistical models, dynamical models, and empirical analyses (e.g., Penland and Sardeshmukh 1995; Kessler 2002; Fedorov et al. 2003; Chen et al. 2004). While one cannot unambiguously determine the stability characteristics of ENSO from a single El Niño case study, characterizing episodic atmospheric forcing observed during the 2002/03 El Niño can provide valuable insights into the nature of the ENSO cycle.

EPISODIC ATMOSPHERIC FORCING. Onset of the 2002/03 El Niño was associated with multiple strong episodic westerly wind events in the western and central Pacific, particularly those in May and June 2002. These events were but two of nine that occurred in 2002. For the year as a whole, 2002 experienced more westerly wind events with zonal anomalies $> 2 \text{ m s}^{-1}$ than any year since 1997 (Table 1). Also, the zonal fetch of the wind events was generally larger in 2002 than in any year since 1997, with the May event extending all the way to 140°W . Nine westerly events also occurred in 1997 in association with the 1997/98 El Niño, but they were generally stronger and extended farther east. Thus, Table 1 suggests that there is a linkage between the frequency, intensity and zonal fetch of episodic westerly forcing and the occurrence and amplitude of El Niño.

Much of the episodic westerly wind forcing in the western and central Pacific immediately prior to and during the 2002/03 El Niño was associated with the MJO, a wavelike atmospheric phenomenon with periods of roughly 30–60 days generated over the Indian Ocean (Madden and Julian 1994). Typically, convective flare-ups associated with the active phase of the MJO propagate eastward toward the western Pacific, affecting surface winds, cloudiness, and precipitation fields over the warm pool. As the MJO, which wraps

around the globe at upper elevations of the atmosphere (one wavelength per earth circumference), propagates farther eastward over the cooler waters of the eastern equatorial Pacific, the surface atmospheric boundary layer stabilizes and becomes decoupled from the free atmosphere. Convection weakens, and the strong local air–sea coupling like that occurring over the western Pacific warm pool is no longer evident.

These characteristics of the MJO and its effects on cloudiness and surface winds were manifest in data from the 2002/03 El Niño. Several convective flare-ups in the Indian Ocean followed by eastward propagation in the western Pacific were evident between July 2001 and July 2002. Several additional propagating convective events were evident between November 2002 and September 2003 (Fig. 9). Each one of these flare-ups was associated with anomalous westerly surface winds in the western Pacific (Figs. 2 and 3), while both convection and surface wind anomalies weakened over the cooler waters of the eastern Pacific. Noteworthy were the MJO events in Fig. 9 labeled A–D, which were associated with the December 2001, May 2002, June–July 2002, and May 2003 westerly wind episodes, respectively. However, there is not always a one-to-one correspondence between MJO convective events and surface westerly anomalies in the western Pacific, with more of the latter than the former. This suggests that the MJO was a prominent but not exclusive cause for episodic westerly wind forcing during the 2002/03 El Niño.

A notable feature of this intraseasonal atmospheric variability was that once El Niño warming was initiated across the basin in May–June 2002, the MJO-related convection appeared to weaken (Fig. 9). Eastward-propagating convective anomalies were less apparent in cloudiness and rainfall over the Indian

TABLE 1. Statistics of westerly wind events based on zonal wind anomalies (U_o) averaged between 2°N and 2°S in the Pacific. Shown are the number of westerly events with anomalies $\geq 2 \text{ m s}^{-1}$ and a minimum fetch of 10° of longitude extending to at least 150°E for each year from 1997 to 2003. Also shown for each year are the maximum westerly anomaly (to the nearest m s^{-1}) and the easternmost longitude (to the nearest 10°) for these westerly wind events. The statistics are based on a gridded analysis of daily TAO/TRITON time series data block averaged every 5 days, then smoothed with a 1–2–1 filter in time (q.v. Fig. 3a).

	1997	1998	1999	2000	2001	2002	2003*
No. of westerly events with $U_o \geq 2 \text{ m s}^{-1}$	9	0	2	4	7	9	6
U_o max (m s^{-1})	11	—	4	4	6	7	5
Easternmost longitude of $U_o \geq 2 \text{ m s}^{-1}$	120°W	—	150°E	150°E	160°W	140°W	160°W

*Data for 2003 are through September only.

OLR Anomaly (5°N to 5°S)

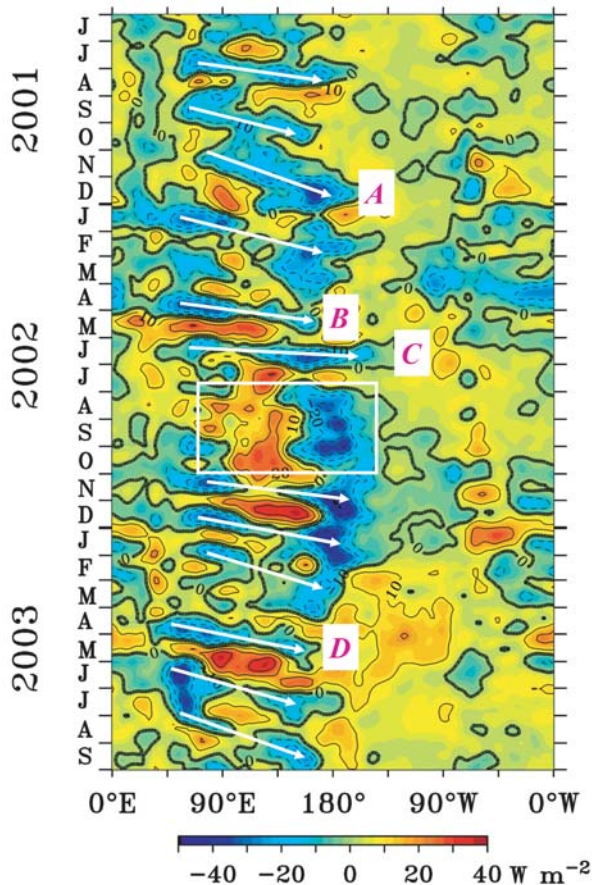


FIG. 9. Five-day OLR anomalies averaged over 5°N–5°S around the globe. Negative values represent anomalously high cloudiness and rainfall associated with disturbed weather conditions, while positive values represent clearer skies and generally drier conditions. Anomalies are relative to a 1979–95 climatology. Arrows indicate eastward-propagating convective events originating over the Indian Ocean. These events are associated with active phases of the MJO and surface westerly winds in the western Pacific. Events labeled A, B, C, and D are linked to the Dec 2001, May 2002, Jun–Jul 2002, and May 2003 westerly winds bursts, respectively. The boxed area highlights the Aug–Oct 2002 period during which anomalous deep convection became anchored near the international date line. The Indian and Pacific Oceans are separated by Indonesian islands between about 100° and 120°E.

Ocean and western Pacific during August–October 2002 than either before or after. Yet anomalous deep convection became anchored near the date line while surface zonal wind and SST anomalies continued to intensify (Fig. 3). These observations suggest that episodic forcing associated with the MJO helped to “kick-start” the 2002/03 El Niño, but that once underway,

large-scale ocean–atmosphere interactions like those described in Sidebar 1 propelled the system toward further warming.

SUMMARY AND DISCUSSION. In situ and satellite observations from the ENSO Observing System underscore the role played by both episodic atmospheric forcing and large-scale low-frequency ocean–atmosphere dynamics in the genesis and evolution of the 2002/03 El Niño. Two to three seasons prior to the onset of the El Niño, there was a buildup in heat content along the equator that preconditioned the system toward the occurrence of a warm event. However, this heat content buildup was similar to that in early 2000 and 2001, which were not El Niño years. It appears that strong episodic westerly wind forcing, particularly that in May–July 2002, was instrumental in initiating the 2002/03 El Niño. This episodic forcing was related to the MJO, a wavelike atmospheric phenomenon generated over the Indian Ocean with periods of roughly 30–60 days. Once the El Niño was underway in the boreal summer of 2002, convection associated with the MJO appeared to weaken for several months while large-scale ocean–atmosphere feedbacks became more fully engaged to amplify and sustain the El Niño warming.

The 2002/03 El Niño reached its maximum development in October–December 2002 in terms of SST, wind, and eastern Pacific thermocline depth anomalies, and in January 2003 in terms of anomalous equatorial deep convection and rainfall. This phasing relative to the mean seasonal cycle is typical of most El Niños (Rasmusson and Carpenter 1982; Harrison and Larkin 1998). The pattern of SST anomalies was unusual, however, with the largest anomalies concentrated in the central equatorial Pacific in contrast to relatively weak and short-lived warming in the eastern Pacific and along the west coasts of the Americas. Precisely what accounted for this SST anomaly pattern is unclear. Anomalous easterly wind stresses along the equator in the eastern and central Pacific (Fig. 5b) were unusual in that typically, they are confined to the east of 100°–120°W during El Niño. The greater zonal extent of anomalous easterly stresses during the 2002/03 El Niño may have partially counteracted the tendency for remote forcing to deepen the thermocline in the eastern basin, leading to weaker SST anomalies than would otherwise have been expected there. Barrier layer effects may also have amplified warming in the central Pacific to enhance zonal asymmetries in the SST anomaly field. A complete understanding of factors giving rise to this unusual SST pattern will require a quantitative evalu-

ation of physical processes from a coupled ocean–atmosphere perspective.

Like most El Niños (Rasmusson and Carpenter 1982; Harrison and Larkin 1998), the 2002/03 El Niño terminated in the boreal spring as anomalies from the previous autumn and winter weakened and largely disappeared. The termination phase of the event through May 2003 involved a combination of western boundary reflection of upwelling equatorial Rossby waves, directly wind-forced upwelling Kelvin waves, and contraction of the western Pacific warm pool by anomalously strong westward currents. There is considerable debate over which of these processes is most important during the demise of El Niño events (e.g., Vialard et al. 2001; Picaut et al. 2002; Boulanger et al. 2003). Efforts are already underway to test different hypotheses with the extensive datasets collected from the ENSO Observing System (e.g., Vecchi and Harrison 2003).

A surprising development in boreal spring 2003 was the aborted cooling trend that had prompted some forecasters to predict the onset of La Niña. This abrupt turnabout of events was in sharp contrast to the termination of the 1997/98 El Niño in which SSTs plummeted 8°C in the equatorial cold tongue during May–June 1998 to usher in 3 yr of persistent La Niña conditions (McPhaden 1999). The sudden reversal of the SST cooling trend in May–June 2003 was the result of MJO-related episodic westerly wind forcing.

Lau and Chan (1986) were the first to suggest that the MJO was a factor in the evolution of El Niño events, arguing the case specifically for the 1982/83 El Niño. The MJO has since been implicated in the development of other events and in particular played a major role in the evolution of the 1997/98 El Niño (McPhaden 1999; Takayabu et al. 1999). Plausible physical mechanisms by which higher-frequency dynamics associated with the MJO can influence ENSO have been described (Kessler et al. 1995; Kessler and Kleeman 2000; Bergman et al. 2001; Zhang 2001). However, the influence of the MJO on ENSO remains a controversial topic. The MJO is active every year and statistical relationships between commonly used ENSO and MJO indices do not provide a convincing argument that the two are causally related (Slingo et al. 1999). This lack of consistency in part may reflect the role that other forms of stochastic forcing can play in the ENSO cycle such as non-MJO-related westerly wind bursts, western tropical Pacific cyclones, and cold air outbreaks from higher latitudes. Lack of a convincing statistical relationship between ENSO and MJO variability may also reflect the role that large-scale dynamics plays in establishing condi-

tions favorable for episodic forcing to be effective and/or to the use of MJO indices that do not fully capture the essential ocean–atmosphere interactions linking the MJO to ENSO (Zhang et al. 2001; Kessler 2001). Nonetheless, the MJO and episodic surface westerly wind forcing associated with it appears to have had a significant influence on the onset, development, and termination phases of the 2002/03 El Niño.

The relationship between the 2002/03 El Niño and episodic westerly forcing, particularly that related to the MJO, raises a number of interesting questions. For example, what were the specific nonlinear oceanic and atmospheric processes that rectified the westerly wind forcing in May–July 2002 into sustained warming? Why did the December 2001 westerly wind event and subsequent Kelvin wave–induced warming in February–March 2002 not lead immediately to the onset of the El Niño? Why did anomalous convective activity associated with the MJO weaken in the Pacific in August–October 2002? Westerly winds events were significantly stronger during the 1997/98 El Niño than during the 2002/03 El Niño. Also, they were less frequent, generally weaker, and of less extensive zonal fetch in the cool years between these El Niños. Are these yearly differences in the statistics of episodic westerly wind events and the MJO controlled by random variations in internal atmospheric dynamics, by underlying interannual Indo-Pacific SST variations, or by a combination of these factors (e.g., Hendon et al. 1999; Kessler 2001)? Finally, would the 2002/03 El Niño have occurred without MJO-related or other episodic westerly wind forcing, as would be the case if ENSO resulted from unstable ocean–atmosphere interactions? If so, how would it have evolved?

Interaction of ENSO with decadal time-scale phenomena may also be important for understanding the details of what transpired during both the 2002/03 El Niño and the prolonged cold period (mid-1998 to 2001) leading up to it. Changes in large-scale background conditions can affect the variability and predictability of ENSO (Power et al. 1999; Fedorov and Philander 2000), and these background conditions are in part related to the phase of the Pacific decadal oscillation (PDO; Mantua et al. 1997). There is evidence to suggest that the PDO may have switched sign from a high phase (weak trade winds, warm Tropics, and warm coastal Americas) to a low phase (strong trade winds, cold Tropics, and cold coastal Americas) in the late 1990s (Chavez et al. 2003; Peterson and Schwing 2003). It is plausible that stronger trade winds and a cooler cold tongue in the tropical Pacific might favor weaker ENSO warm events and stronger ENSO cold events on average relative to the previous 25 yr of

PDO warm-phase conditions. Precisely how ENSO interacts with the PDO and other modes of decadal variability in the Pacific remains an open question though. Indeed, there is even uncertainty as to whether the decadal modulation of ENSO is the cause of, or the consequence of, variations in the background state of the tropical Pacific (e.g., Kirtman and Shopf 1998).

As one measure of progress in ENSO forecasting, several models in early 2002 predicted that the year would be unusually warm (Kerr 2002). However, there was considerable spread in ENSO forecasts during early 2002, with some predicting near-neutral or cold conditions in the tropical Pacific over the next two to three seasons (Kirtman 2002). Also, most models underpredicted the strength of warm Niño-3.4 SST anomalies from forecasts issued in the first half of 2002 even after initial warming developed (<http://iri.columbia.edu/climate/ENSO/currentinfo/archive/>). Model biases and/or inadequate specification of initial conditions may have contributed to these forecast errors. In addition, the occurrence of episodic westerly wind forcing, much of which was associated with MJO variability, was also a factor in limiting forecast skill. Most atmospheric circulation models used in dynamical forecasting schemes do not simulate the MJO well, if at all. Statistical ENSO forecast models, trained on seasonally averaged conditions over many ENSO cycles, are not particularly sensitive to short-lived episodic atmospheric fluctuations. These fluctuations, which represent unpredictable noise on seasonal time scales, had a significant influence on the character of the 2002/03 El Niño.

The uniqueness of the 2002/03 El Niño illustrates the point that no two El Niños are exactly alike and that event-to-event differences can have significant socioeconomic consequences. For instance, warming in the eastern Pacific and along the northwest coast of South America in March 2002 brought torrential rains to parts of Ecuador and northern Peru, causing severe flooding, agricultural losses, and fatalities. Some scientists at the time argued that these rains should not be attributed to El Niño since the warming was associated with the passage of a transient intraseasonal Kelvin wave (Fig. 2). Also, previous “false positive” El Niño warmings had occurred briefly in the eastern equatorial Pacific in early 2000 and early 2001 (the latter of which can be seen in Fig. 3b). Thus, as noted in the introduction, there was no clear consensus in March 2002 that an El Niño was underway.

Once basin-scale warming along the equator became evident in mid-2002, there was heightened interest in forecasts of the subsequent growth and ulti-

mate strength of the El Niño. Most early advisories calling for a weak or weak-to-moderate warm event were cautious because of the significant spread in model forecasts at two–three-season lead times. As the event progressed, though, the governments of Peru and Ecuador invested considerable effort in preparing their countries for potential El Niño–related natural disasters, mindful of the destruction wrought by the recent 1997/98 El Niño. In particular, there was an expectation for heavy rains in the coastal zone where El Niño typically has a strong impact early in the calendar year. However, the lack of prolonged anomalous warming in the eastern Pacific in early 2003 led to unexpected dryness in Peru and Ecuador during what is normally considered the rainy season. Some areas typically affected by heavy El Niño rainfalls even experienced severe drought. While the region was spared from flooding and other disasters that typically accompany El Niño occurrences, the forecast for increased probability of above-normal precipitation nonetheless created significant economic hardship. The agricultural sector was particularly hard hit since planting strategies for many crops were predicated on the expectation of wetter climatic conditions than actually materialized.

This example (and others that could be cited) highlights the need to reduce uncertainties in ENSO forecasts so that they can be used with more confidence as a decision support tool. Great strides have been made over the past 20 yr in developing ENSO forecast models that have some skill in predicting whether the tropical Pacific will be unusually warm or cold up to a year in advance and in incorporating this information into long range weather forecasts. However, there is much room for improvement in our ability to predict the details of individual El Niño and La Niña events and their climatic consequences both globally and regionally. The ENSO puzzle thus continues to challenge climate research and forecasting communities, not only because it is a compelling scientific problem, but also because of its widespread socioeconomic impacts.

ACKNOWLEDGMENTS. The author would like to thank Billy Kessler of NOAA’s Pacific Marine Environmental Laboratory (PMEL) and Sophie Cravatte of the Laboratoire d’Etudes en Géophysique et Oceanographie Spatiale in Toulouse, France, for comments on an earlier version of this manuscript. Special thanks also to Gary Lagerloef of Earth and Space Research for access to surface velocity analyses of the Ocean Surface Current Analyses-Real Time (OSCAR) project and to Gary Mitchum of the University of South Florida for access to his analysis of

merged TOPEX/Poseidon and Jason satellite altimeter data. Captain Rodney Martinez of the Instituto Oceanografico de la Armada in Guayaquil, Ecuador, and Dr. Renato Guevara-Carrasco, Science Director of the Instituto del Mar del Peru in Callao, Peru, provided valuable information on the effects of the 2002/03 El Niño in their countries. The comments of three anonymous reviewers led to significant improvements in the quality of this manuscript. Margie McCarty and Dai McClurg of NOAA/PMEL and the Joint Institute for the Study of the Atmosphere and Ocean (JISAO) at the University of Washington generated the graphics for this paper. Production of this manuscript was supported by NOAA's Office of Oceanic and Atmospheric Research, NOAA's Office of Global Programs, and JISAO under NOAA Cooperative Agreement NA17RJ1232.

REFERENCES

- Ando, K., and M. J. McPhaden, 1997: Variability of surface layer hydrography in the tropical Pacific Ocean. *J. Geophys. Res.*, **102**, 23 063–23 078.
- Argo Science Team, 2001: The global array of profiling floats. *Observing the Ocean in the 21st Century*. C. J. Koblinsky and N. R. Smith, Eds., Australian Bureau of Meteorology, 248–258.
- Barber, R. T., and F. P. Chavez, 1983: Biological consequences of El Niño. *Science*, **222**, 1203–1210.
- Barnston, A. G., Y. He, and M. H. Glantz, 1999: Predictive skill of statistical and dynamical climate models in SST forecasts during the 1997–98 El Niño episode and the 1998 La Niña onset. *Bull. Amer. Meteor. Soc.*, **80**, 217–244.
- Battisti, D. S., 1988: Dynamics and thermodynamics of a warming event in a coupled atmosphere–ocean model. *J. Atmos. Sci.*, **45**, 2889–2919.
- Ballabrera-Poy, J., R. Murtugudde, and A. J. Busalacchi, 2002: On the potential impact of sea surface salinity observation on ENSO predictions. *J. Geophys. Res.*, **107**, 8007, doi:10.1029/2001JC000834.
- Bentamy, A., Y. Quilfen, F. Gohin, N. Grima, M. Lenaour, and J. Servain, 1996: Determination and validation of average wind fields from ERS-1 scatterometer measurements. *Global Atmos. Ocean Syst.*, **4**, 1–29.
- Bergman, J. W., H. H. Hendon, and K. M. Weickmann, 2001: Intraseasonal air–sea interactions at the onset of El Niño. *J. Climate*, **14**, 1702–1719.
- Bjerknes, J., 1969: Atmospheric teleconnections from the equatorial Pacific. *Mon. Wea. Rev.*, **97**, 163–172.
- Bonjean, F., and G. S. E. Lagerloef, 2002: Diagnostic model and analysis of the surface currents in the tropical Pacific Ocean. *J. Phys. Oceanogr.*, **32**, 2938–2954.
- Boulanger, J.-P., S. Cravatte, and C. Menkes, 2003: Generation of interannual Kelvin waves in the western Pacific Ocean. *J. Geophys. Res.*, **108**(C10), 3311, doi: 10.1029/2002JC001760.
- Cane, M. A., S. E. Zebiak, and S. C. Dolan, 1986: Experimental forecasts of the 1982/83 El Niño. *Nature*, **321**, 827–832.
- Changnon, S. A., 1999: Impacts of 1997–98 El Niño-generated weather in the United States. *Bull. Amer. Meteor. Soc.*, **80**, 1819–1828.
- Chavez, F. P., P. G. Strutton, G. E. Friederich, R. A. Feely, G. C. Feldman, D. G. Foley, and M. J. McPhaden, 1999: Biological and chemical response of the equatorial Pacific Ocean to the 1997–1998 El Niño. *Science*, **28**, 2126–2131.
- , J. Ryan, S. E. Lluch-Cota, and M. Niquen, 2003: From anchovies to sardines and back: Multidecadal change in the Pacific Ocean. *Science*, **299**, 217–221.
- Chen, D., M. A. Cane, A. Kaplan, S. E. Zebiak, and D. Huang, 2004: Predictability of El Niño over the past 148 years. *Nature*, **428**, 733–736.
- Cronin, M. F., and M. J. McPhaden, 2002: Barrier layer formation during westerly wind bursts. *J. Geophys. Res.*, **107**, 8020, doi:10.1029/2001JC001171.
- Delcroix, T., and J. Picaut, 1998: Zonal displacement of the western equatorial Pacific fresh pool. *J. Geophys. Res.*, **103**, 1087–1098.
- , and M. J. McPhaden, 2002: Interannual sea surface salinity and temperature changes in the western Pacific warm pool during 1992–2000. *J. Geophys. Res.*, **107**, 8002, doi:10.1029/2001JC000862.
- Eckert, C., and M. Latif, 1997: Predictability of a stochastically forced hybrid coupled model of El Niño. *J. Climate*, **10**, 1488–1504.
- Fedorov, A. V., and S. G. Philander, 2000: Is El Niño changing? *Science*, **288**, 1997–2001.
- , S. L. Harper, S. G. Philander, B. Winter, and A. Wittenberg, 2003: How predictable is El Niño? *Bull. Amer. Meteor. Soc.*, **84**, 911–919.
- Feely, R. A., and Coauthors, 2002: Seasonal and interannual variability of CO₂ in the equatorial Pacific. *Deep-Sea Res.*, **49**, 2443–2469.
- Harrison, D. E., and G. A. Vecchi, 1997: Westerly wind events in the tropical Pacific 1986–1995. *J. Climate*, **10**, 3131–3156.
- , and N. A. Larkin, 1998: El Niño–Southern Oscillation sea surface temperature and wind anomalies, 1946–1993. *Rev. Geophys.*, **36**, 353–399.
- , and G. A. Vecchi, 1999: On the termination of El Niño. *Geophys. Res. Lett.*, **26**, 1593–1596.
- Hendon, H. H., C. Zhang, and J. D. Glick, 1999: Interannual variation of the Madden–Julian oscillation during austral summer. *J. Climate*, **12**, 2538–2550.

- Janowiak, J. E., and P. Xie, 1999: CAMS_OPI: A global satellite–rain gauge merged product for real-time precipitation monitoring applications. *J. Climate*, **12**, 3335–3342.
- Jin, F. F., 1997: An equatorial recharge paradigm for ENSO. Part I: Conceptual model. *J. Atmos. Sci.*, **54**, 811–829.
- Keen, R. A., 1982: The role of cross-equatorial tropical cyclone pairs in the Southern Oscillation. *Mon. Wea. Rev.*, **110**, 1405–1416.
- Kerr, R., 2002: Signs of success in forecasting El Niño. *Science*, **97**, 497–498.
- Kessler, W. S., 2001: EOF representation of the Madden–Julian oscillation and its connection with ENSO. *J. Climate*, **14**, 3055–3061.
- , 2002: Is ENSO a cycle or a series of events? *Geophys. Res. Lett.*, **29**, 2125–2128.
- , and R. Kleeman, 2000: Rectification of the Madden–Julian oscillation into the ENSO cycle. *J. Climate*, **13**, 3560–3575.
- , M. J. McPhaden, and K. M. Weickmann, 1995: Forcing of intraseasonal Kelvin waves in the equatorial Pacific. *J. Geophys. Res.*, **100**, 10 613–10 631.
- Kirtman, B. P., Ed., 2002: *Experimental Long-Lead Forecast Bulletin*. Vol. 11, No. 1, Center for Ocean–Land–Atmosphere Studies, Calverton, MD, 57 pp. [Available online at <http://www.iges.org/ellfb>.]
- , and P. S. Schopf, 1998: Decadal variability in ENSO predictability and prediction. *J. Climate*, **11**, 2804–2822.
- Kleeman, R., and S. B. Power, 1994: Limits to predictability in a coupled ocean–atmosphere model due to atmospheric noise. *Tellus*, **46A**, 529–540.
- Lagerloef, G. S. E., G. T. Mitchum, R. Lukas, and P. P. Niiler, 1999: Tropical Pacific near surface currents estimated from altimeter, wind, and drifter data. *J. Geophys. Res.*, **104**, 23 313–23 326.
- , R. Lukas, F. Bonjean, J. T. Gunn, G. T. Mitchum, M. Bourassa, and A. J. Busalacchi, 2003: El Niño tropical Pacific Ocean surface current and temperature evolution in 2002 and outlook for early 2003. *Geophys. Res. Lett.*, **30**, 1514, doi:10.1029/2003GL017096.
- Landsea, C. W., and J. A. Knaff, 2000: How much skill was there in forecasting the very strong 1997–98 El Niño? *Bull. Amer. Meteor. Soc.*, **81**, 2107–2120.
- Lau, K.-M., and P. H. Chan, 1986: The 40–50 day oscillation and the El Niño/Southern Oscillation: A new perspective. *Bull. Amer. Meteor. Soc.*, **67**, 533–534.
- Lehody, P., M. Betignac, J. Hampton, A. Lewis, and J. Picaut, 1997: El Niño Southern Oscillation and tuna in the western Pacific. *Nature*, **389**, 715–718.
- Lukas, R., and E. Lindstrom, 1991: The mixed layer in the western equatorial Pacific Ocean. *J. Geophys. Res.*, **96**, 3343–3357.
- Madden, R. A., and P. R. Julian, 1994: Observations of the 40–50-day tropical oscillation—A review. *Mon. Wea. Rev.*, **122**, 814–837.
- Maes, C., J. Picaut, and S. Belamari, 2002: Salinity barrier layer in onset of El Niño in a coupled model. *Geophys. Res. Lett.*, **29**, 2206, doi: 10.1029/2002GL016029.
- Mantua, N. J., S. J. Hare, Y. Zhang, J. M. Wallace, and R. C. Francis, 1997: A Pacific interdecadal oscillation with impacts on salmon production. *Bull. Amer. Meteor. Soc.*, **78**, 1069–1079.
- Mason, S. J., L. Goddard, N. E. Graham, E. Yulaeva, L. Sun, and P. A. Arkin, 1999: The IRI seasonal climate prediction system and the 1997/98 El Niño event. *Bull. Amer. Meteor.*, **80**, 1853–1874.
- McPhaden, M. J., 1999: Genesis and evolution of the 1997–98 El Niño. *Science*, **283**, 950–954.
- , and X. Yu, 1999: Equatorial waves and the 1997–98 El Niño. *Geophys. Res. Lett.*, **26**, 2961–2964.
- , T. Delcroix, K. Hanawa, Y. Kuroda, G. Meyers, J. Picaut, and M. Swenson, 2001: The El Niño/Southern Oscillation (ENSO) Observing System. *Observing the Ocean in the 21st Century*, C. J. Koblinky and N. R. Smith, Eds., Australian Bureau of Meteorology, 231–246.
- Meinen, C. S., and M. J. McPhaden, 2000: Observations of warm water volume changes in the equatorial Pacific and their relationship to El Niño and La Niña. *J. Climate*, **13**, 3551–3559.
- Moore, A. M., and R. Kleeman, 1999: Stochastic forcing of ENSO by the intraseasonal oscillation. *J. Climate*, **12**, 1199–1220.
- Neelin, J. D., D. S. Battisti, A. C. Hirst, F.-F. Jin, Y. Wakata, T. Yamagata, and S. Zebiak, 1998: ENSO theory. *J. Geophys. Res.*, **103**, 14 261–14 290.
- Office of Global Programs, 1999: An experiment in the application of climate forecasts: NOAA-OGP activities related to the 1997–98 El Niño event. NOAA Office of Global Programs, 134 pp.
- Page, S. E., F. Siegart, J. O. Reiley, H.-D. V. Boehm, A. Jaya, and W. Limin, 2002: The amount of carbon released from peat and forest fires in Indonesia during 1997. *Nature*, **420**, 61–65.
- Pegion, P. J., M. A. Bourassa, D. M. Legler, and J. J. O’Brien, 2000: Objectively derived daily “winds” from satellite scatterometer data. *Mon. Wea. Rev.*, **128**, 3150–3168.
- Penland, C., and P. D. Sardeshmukh, 1995: The optimal growth of tropical sea surface temperature anomalies. *J. Climate*, **8**, 1999–2024.

- Peterson, W. T., and F. B. Schwing, 2003: A new climate regime in the northeast Pacific Ocean. *Geophys. Res. Lett.*, **30**, 1896, doi:10.1029/2003GL017528.
- Picaut, J., M. Ioualalen, C. Menkes, T. Delcroix, and M. J. McPhaden, 1996: Mechanism of the zonal displacements of the Pacific warm pool: Implications for ENSO. *Science*, **274**, 1486–1489.
- , F. Masia, and Y. du Penhoat, 1997: An advective-reflective conceptual model for the oscillatory nature of ENSO. *Science*, **277**, 663–666.
- , E. Hackert, A. J. Busalacchi, R. Murtugudde, and G. S. E. Lagerloef, 2002: Mechanisms of the 1997–1998 El Niño–La Niña, as inferred from space-based observations. *J. Geophys. Res.*, **107**, 3037, doi:10.1029/2001JC000850.
- Pielke, R. A., Jr., and C. N. Landsea, 1999: La Niña, El Niño, and hurricane damages in the United States. *Bull. Amer. Meteor. Soc.*, **80**, 2027–2033.
- Power, S., C. Folland, A. Colman, and V. Mehta, 1999: Interdecadal modulation of the impact of ENSO on Australia. *Climate Dyn.*, **15**, 319–324.
- Rasmusson, E. M., and T. H. Carpenter, 1982: Variations in tropical sea surface temperature and surface wind fields associated with the Southern Oscillation/El Niño. *Mon. Wea. Rev.*, **110**, 354–384.
- , and J. M. Wallace, 1983: Meteorological aspects of the El Niño/Southern Oscillation. *Science*, **222**, 1195–1202.
- Reynolds, R. W., N. A. Rayner, T. M. Smith, D. C. Stokes, and W. Wang, 2002: An improved in situ and satellite SST analysis for climate. *J. Climate*, **15**, 1609–1625.
- Schopf, P. S., and M. J. Suarez, 1988: Vacillations in a coupled ocean–atmosphere model. *J. Atmos. Sci.*, **45**, 549–566.
- Slingo, J. M., D. P. Powell, K. R. Sperber, and F. Nortley, 1999: On the predictability of the interannual behavior of the Madden–Julian oscillation and its relation to ENSO. *Quart. J. Roy. Meteor. Soc.*, **125**, 583–609.
- Smith, N. R., 1995: An improved system for tropical ocean subsurface temperature analyses. *J. Atmos. Oceanic Technol.*, **12**, 850–870.
- Takayabu, Y. N., T. Iguchi, M. Kachi, A. Shibata, and H. Kanzawa, 1999: Abrupt termination of the 1997–98 El Niño in response to a Madden–Julian oscillation. *Nature*, **402**, 279–282.
- Trenberth, K. E., G. W. Branstator, D. Karoly, A. Kumar, N.-C. Lau, and C. Ropelewski, 1998: Progress during TOGA in understanding and modeling global teleconnections associated with tropical sea surface temperatures. *J. Geophys. Res.*, **103**, 14 291–14 324.
- Vecchi, G. A., and D. E. Harrison, 2003: On the termination of the 2002–03 El Niño event. *Geophys. Res. Lett.*, **30**(18), 1964, doi:10.1029/2003GL017564.
- Vialard, J., C. Menkes, J.-P. Boulanger, P. Delecluse, E. Guilyardi, M. J. McPhaden, and G. Madec, 2001: A model study of oceanic mechanisms affecting equatorial Pacific sea surface temperature during the 1997–98 El Niño. *J. Phys. Oceanogr.*, **31**, 1649–1675.
- Weisberg, R. H., and C. Wang, 1997: A western Pacific oscillator paradigm for the El Niño–Southern Oscillation. *Geophys. Res. Lett.*, **24**, 779–782.
- Weller, R. A., and S. P. Anderson, 1996: Surface meteorology and air–sea fluxes in the western equatorial Pacific warm pool during TOGA COARE. *J. Climate*, **9**, 1959–1990.
- Woodruff, S. D., R. J. Slutz, R. L. Jenne, and P. Steurer, 1987: A comprehensive ocean–atmosphere data set. *Bull. Amer. Meteor. Soc.*, **68**, 1239–1250.
- Wyrtki, K., 1985: Water displacements in the Pacific and the genesis of El Niño cycles. *J. Geophys. Res.*, **90**, 7129–7132.
- Xue, Y., T. M. Smith, and R. W. Reynolds, 2003: Interdecadal changes of 30-yr SST normals during 1871–2000. *J. Climate*, **16**, 1601–1612.
- Yu, L., and M. M. Reinecker, 1998: Evidence of an extratropical influence during the onset of the 1997–98 El Niño. *Geophys. Res. Lett.*, **25**, 3537–3540.
- Zebiak, S., 1989: Oceanic heat content variability and El Niño cycles. *J. Phys. Oceanogr.*, **19**, 475–486.
- Zhang, C., 2001: Intraseasonal perturbations in sea surface temperatures of the equatorial eastern Pacific and their association with the Madden–Julian oscillation. *J. Climate*, **14**, 1309–1322.
- , H. H. Hendon, W. S. Kessler, and A. J. Rosati, 2001: A workshop on the MJO and ENSO. *Bull. Amer. Meteor. Soc.*, **82**, 971–976.